Osteoactivin upregulates expression of MMP-3 and MMP-9 in fibroblasts infiltrated into denervated skeletal muscle in mice

Takayuki Ogawa, Takeshi Nikawa, Harumi Furochi, Miki Kosyoji, Katsuya Hirasaka, Naoto Suzue, Koichi Sairyo, Shunji Nakano, Takashi Yamaoka, Mitsuo Itakura, Kyoichi Kishi and Natsuo Yasui

Am J Physiol Cell Physiol 289:697-707, 2005. doi:10.1152/ajpcell.00565.2004

Am J Physiol Cell Physiol 289: C697–C707, 2005;
doi:10.1152/ajpcell.00565.2004.

Osteoactivin upregulates expression of MMP-3 and MMP-9 in fibroblasts infiltrated into denervated skeletal muscle in mice

Takayuki Ogawa,[1] Takeshi Nikawa,[2] Harumi Furochi,[2] Miki Kosyoji,[2] Katsuya Hirasaka,[2] Naoto Suzue,[1] Koichi Sairyo,[1] Shunji Nakano,[1] Takashi Yamaoka,[3] Mitsuo Itakura,[3] Kyoichi Kishi,[2] and Natsuo Yasui[1]

[1]*Department of Orthopaedics and* [2]*Department of Nutrition, The University of Tokushima School of Medicine,* [3]*Division of Genetic Information, Institute for Genome Research, The University of Tokushima, Tokushima, Japan*

Submitted 22 November 2004; accepted in final form 7 April 2005

Ogawa, Takayuki, Takeshi Nikawa, Harumi Furochi, Miki Kosyoji, Katsuya Hirasaka, Naoto Suzue, Koichi Sairyo, Shunji Nakano, Takashi Yamaoka, Mitsuo Itakura, Kyoichi Kishi, and Natsuo Yasui. Osteoactivin upregulates expression of MMP-3 and MMP-9 in fibroblasts infiltrated into denervated skeletal muscle in mice. *Am J Physiol Cell Physiol* 289: C697–C707, 2005; doi:10.1152/ajpcell.00565.2004.—In this study, we examined pathophysiological roles of osteoactivin, a functionally unknown type I membrane glycoprotein, in mouse skeletal muscle atrophied by denervation (sciatic neurectomy). Denervation increased the amounts of osteoactivin, vimentin, matrix metalloproteinase-3 (MMP-3), and MMP-9 in mouse gastrocnemius muscle. Interestingly, immunohistochemical analysis revealed that vimentin, MMP-3, and MMP-9 were mainly present in fibroblast-like cells infiltrated into denervated mouse gastrocnemius muscle, whereas osteoactivin was expressed in the sarcolemma of myofibers adjacent to the fibroblast-like cells. On the basis of these findings, we reasoned that osteoactivin in myocytes was involved in activation of the infiltrated fibroblasts. To address this issue, we examined effects of osteoactivin on expression of MMPs in fibroblasts in vitro and in vivo. Overexpression of osteoactivin in NIH-3T3 fibroblasts induced expression of MMP-3, but not in mouse C_2C_{12} myoblasts, indicating that osteoactivin might functionally target fibroblasts. Treatment with recombinant mouse osteoactivin increased the amounts of collagen type I, MMP-3, and MMP-9 in mouse NIH-3T3 fibroblasts. The upregulated expression of these fibroblast marker proteins was significantly inhibited by heparin, but not by an integrin inhibitor, indicating that a heparin-binding motif in the extracellular domain might be an active site of osteoactivin. In osteoactivin-transgenic mice, denervation further enhanced expression of MMP-3 and MMP-9 in fibroblasts infiltrated into gastrocnemius muscle, compared with wild-type mice. Our present results suggest that osteoactivin might function as an activator for fibroblasts infiltrated into denervated skeletal muscles and play an important role in regulating degeneration/regeneration of extracellular matrix.

sciatic neurectomy; Gpnmb family; C_2C_{12} cells; NIH-3T3 cells; osteoactivin-transgenic mice

DENERVATION (sciatic neurectomy) causes numerous changes in contractile, electrical, metabolic, and molecular properties of the muscle fiber membrane and sarcoplasm in hindlimb skeletal muscles (6, 10). Previous studies (21, 22, 32) have shown evidence that denervation alters interstitial spaces between muscle fibers: mononucleated cells are infiltrated into interstitial spaces of muscle fibers, and fibrosis occasionally occurs in the muscle. These findings suggest that the interaction between muscle fiber membrane and infiltrated cells might play an important role in degeneration or regeneration of denervated skeletal muscle. However, information on the interaction between the muscle fiber membrane and infiltrated cells is very little.

To address this issue, we previously examined the expression of ~26,000 genes in rat gastrocnemius muscle atrophied by denervation or spaceflight using an Affymetrix DNA microarray analytical system (25). We found that both conditions remarkably increased the expression of osteoactivin, a functionally unknown type I membrane glycoprotein, in skeletal muscle. Besides being an EST gene (AA818039), the osteoactivin gene was only a transcript, whose expression was upregulated more than eightfold by spaceflight and denervation (25).

Osteoactivin is a rat homolog of Gpnmb family, which was originally reported to be highly expressed in human melanoma cells (36). Recently, osteoactivin transcripts have been reported to increase in various diseases associated with fibrosis, such as osteopetrosis and liver cirrhosis (26, 30). Osteoactivin has several interesting binding motifs for extracellular matrix proteins: a heparin-binding motif and an RGD motif for an integrin-binding site (33). On the basis of these findings, we hypothesize that highly expressed osteoactivin might interact with infiltrated cells, such as fibroblasts, leading to the degeneration or regeneration of extracellular matrix in denervated skeletal muscle.

In this study, we examined pathophysiological roles of osteoactivin in the mouse skeletal muscle atrophied by denervation. Immunohistochemical analysis revealed that denervation increased the expression of osteoactivin in muscle fiber membrane, whereas matrix metalloproteinase 3 (MMP-3) and MMP-9 were highly expressed in neighboring fibroblasts. Overexpression of osteoactivin or treatment with its recombinant proteins increased collagen type I, MMP-3, and MMP-9 in mouse NIH-3T3 fibroblasts, but not in mouse C_2C_{12} myoblasts. Moreover, these matrix-related genes were more expressed in fibroblasts infiltrated into denervated skeletal muscles of osteoactivin-transgenic mice, compared with those in wild-type mice. Our present results suggest that the interaction between osteoactivin and fibroblasts stimulates expression of these matrix proteins and that osteoactivin is a key protein for regulating fibroblast functions in the skeletal muscle atrophied by denervation.

MATERIALS AND METHODS

Denervation and tail suspension. Adult male (C57BL/6xDBA/2) F1 (BDF1) mice (~9 wk old), weighing 18–22 g, were purchased

Address for reprint requests and other correspondence: T. Nikawa, Dept. of Nutrition, The Univ. of Tokushima School of Medicine, 3-18-15 Kuramoto-cho, Tokushima 770-8503, Japan (e-mail: nikawa@nutr.med.tokushima-u.ac.jp).

The costs of publication of this article were defrayed in part by the payment of page charges. The article must therefore be hereby marked "*advertisement*" in accordance with 18 U.S.C. Section 1734 solely to indicate this fact.

from Japan SLC (Shizuoka, Japan). The mice were housed in a room maintained at 23 ± 2°C on a 12:12-h light-dark cycle and allowed free access to food and water. All protocols were performed according to the Guide for the Care and Use of Laboratory Animals at The University of Tokushima. The experiments performed in this study were approved by the Animal Care and Use Committee of the University of Tokushima School of Medicine.

For the denervation procedure, the dorsal skin of the right thigh was cut and the posterior muscles were divided to show the sciatic nerve. Chronic denervation was caused by removal of a sciatic nerve section of 5 mm in length (23). In the tail suspension procedure, a piece of tape was attached on the tail, and this tape was connected to a swivel tied to a horizontal bar at the top of the cage (37). Control animals were prepared in a parallel procedure. The hindlimb skeletal muscles, such as gastrocnemius, soleus, and tibialis anterior muscles, were isolated at the indicated times. After the wet weight was measured, the skeletal muscles were immediately frozen in chilled isopentane and liquid nitrogen and were stored at −80°C until analysis.

Cell culture. Mouse myoblastic C_2C_{12} cells were purchased from Dainippon Pharmaceutical (Osaka, Japan). Mouse fibroblastic NIH-3T3 cells were a kind gift from Dr. N. Harada of The University of Tokushima School of Medicine, Tokushima, Japan. The cells were maintained and proliferated at 37°C with 5% CO_2-95% air in Dulbecco's modified Eagle's medium, supplemented with 10% fetal calf serum, 100 U/ml penicillin, and 0.1 mg/ml streptomycin. The first to third passages of cells from the purchased ones were used for the following experiments.

To examine the effects of growth factors on osteoactivin expression, C_2C_{12} cells were treated with 5 ng/ml recombinant human basic fibroblast growth factor (bFGF) (Kaken Pharmaceutical, Tokyo, Japan) in the absence or presence of 300 μg/ml heparin (Sigma, St. Louis, MO), 25 ng/ml platelet-derived growth factor (PDGF) purified from human platelets (Sigma), and 2.5–12.5 ng/ml recombinant human MMP-3 (Sigma), respectively.

Transfection of osteoactivin. We constructed an expression vector for V5/His-tagged mouse osteoactivin by using reverse transcription-polymerase chain reaction (RT-PCR) and cloning techniques as described previously (4, 13). Total RNA was extracted from NIH-3T3 cells with an acid guanidinium thiocyanate-phenol-chloroform mixture (Isogen; Nippon Gene, Tokyo, Japan) according to the standard protocol (5). First-strand cDNAs were reverse transcribed at 37°C for 50 min from 1 μg of the extracted total RNA with oligo-dT15 primer and SuperScript II reverse transcriptase (Invitrogen, Carlsbad, CA). After the initial denaturation at 94°C for 2 min, second-strand synthesis and DNA amplification with Pfx DNA polymerase (Invitrogen) and the osteoactivin primer set (5′-CACCATGGAAAGTCTCTGCGGGGTC-3′ and 5′-GAGTGTCCTTGGCTTGTCCTGGAGC-3′) were accomplished through 30 cycles of the following incubations: 15 s at 94°C, 30 s at 60°C, 90 s at 68°C, with the use of a thermal cycler (MJ Research, Watertown, MA). The PCR products were sequenced and cloned into an expression vector pcDNA3.1/V5-His (Invitrogen). For overexpression of osteoactivin in vitro, NIH-3T3 or C_2C_{12} cells were transfected with 2 μg/60-mm dish of the purified plasmid containing osteoactivin (pcDNA3.1/V5-His-tagged osteoactivin) by using FuGene6 (Roche Diagnostics, Mannheim, Germany), according to the method of Hellgren et al. (12).

Generation of osteoactivin-transgenic mice. To express osteoactivin effectively in vivo, the *Bam*HI/*Pme*I fragment of pcDNA3.1/V5-His-tagged osteoactivin was subcloned into an expression vector containing the cytomegalovirus immediate early enhancer chicken β-globin hybrid promoter (31). It provided a transgene cassette composed of the cytomegalovirus promoter and rabbit β-globin exons 2 and 3 linked to V5-His-tagged osteoactivin cDNA. The V5-His-tagged rat osteoactivin cDNA construct was injected into fertilized BDF1 eggs for the production of transgenic mice (Japan SLC). After the most expressed osteoactivin transgenics were back-crossed into BDF1 mice, three strains of heterozygous transgenic mice were generated. Expression of osteoactivin was determined by RT-PCR for osteoactivin and immunobotting for V5 as described below. We maintained the mice under specific pathogen-free conditions, and some of them at 6–12 wk of age were used for experiments.

Treatment with recombinant osteoactivin protein. cDNA encoding mouse osteoactivin (AA22–355) truncated the transmembrane domain was amplified by RT-PCR with the following primer set: 5′-TCCATAAGATTAGCGGATCCTACCTG-3′ and 5′-TCAGACCGCTTCTGCGTTCTGATTTA-3′. The cDNA product was cloned into pBAD/myc-His vector (Invitrogen). The recombinant protein was produced in *Escherichia coli* and purified with a Ni-NTA resin agarose (Invitrogen), according to the standard protocol (29). NIH-3T3 cells with 60% of confluence were treated with 25 nM (final concentration) of the recombinant osteoactivin or *Lac*Z (control) and cultured for the indicated times. In some experiments, 100 μM RGDS peptide, an integrin inhibitor (Sigma), or 300 μg/ml heparin was simultaneously added to NIH-3T3 cells. After being washed with phosphate-buffered saline (PBS), cells were suspended in 50 mM Tris·HCl buffer, pH 7.5, containing 150 mM NaCl, 1% Triton X-100, and 1 tablet of 25-ml protease inhibitor cocktails (Roche Diagnostics).

Preparation of an anti-osteoactivin antibody. Because an anti-osteoactivin antibody was not commercially available, an antiserum against recombinant mouse osteoactivin peptide (AA527–575) fused to glutathione-*S*-transferase (GST) was raised in rabbits. Briefly, the GST-fused osteoactivin peptide was expressed in *E. coli* and purified as described previously (34). Each of two rabbits was immunized with 300 μg of the purified GST-fused osteoactivin peptide in Freund's complete adjuvant (1:1) and monthly boosted. Six months later, blood was collected from the central artery of the ear, and the IgG fraction of the antiserum was prepared by the method of Steinbuch and Audran (35). We further subjected the IgG fraction to affinity column chromatography with HiTrap NHS (Amersham Biosciences, Piscataway, NJ) conjugated with the recombinant osteoactivin peptide (AA527–575). The bound antibody was eluted with 1 mM HCl, immediately neutralized, and stored at 4°C.

Immunoblot analysis. Immunoblot analysis was performed as described previously (13). The whole cell and skeletal muscle extracts (40 μg protein/lane) were subjected to SDS-6, 8, 10, or 12% PAGE and transferred to a polyvinylidene difluoride membrane. The membrane was blocked with 4% skim milk and then incubated with primary antibodies for 1 h at 25°C. The primary antibodies used for the analysis were as follows: polyclonal anti-osteoactivin, polyclonal anti-MMP-2 (Sigma), monoclonal anti-MMP-3 (R&D Systems, Minneapolis, MN), polyclonal anti-MMP-9 (Sigma), polyclonal anti-collagen type I (Santa Cruz Biotechnology), monoclonal anti-V5 (Invitrogen), or anti-β-actin antibody (Oncogene Research Products, San Diego, CA). The bound antibodies were detected with the use of the suitable secondary antibodies and the enhanced chemiluminescence system (Amersham Biosciences). Signals were quantitated by densitometric analysis. We used β-actin as an internal standard protein because the denervation did not change the amount of β-actin. Protein concentrations were determined by Lowry's method with bovine serum albumin as a standard (19).

Histochemical analysis. To examine the localization of osteoactivin or MMP-3 in the denervated gastrocnemius muscle, immunohistochemical analysis was performed. Sections (5 μm) were fixed in ice-cold acetone for 10 min. After being rinsed with PBS three times, the sections were incubated with a 1:100 dilution of monoclonal anti-mouse MMP-3 antibody or polyclonal anti-mouse MMP-9 antibody (Sigma) and a 1:40 dilution of polyclonal anti-osteoactivin antibody at 4°C for 18 h. After being washed with PBS, the sections were incubated with a 1:600 dilution of secondary Alexa 488-conjugated anti-mouse IgG (Molecular Probes, Eugene, OR) and Alexa 568-conjugated anti-rabbit IgG (Molecular Probes) for 1 h at room temperature in the dark. For detection of vimentin, the fixed sections were incubated with a 1:200 dilution of monoclonal anti-human vimentin antibody labeled with Cy3 (Sigma) at 4°C for 18 h. In some

cases, the sections were further incubated with a 1:1,000 dilution of Hoechst-33342 (Dojindo, Kumamoto, Japan) for 10 min at room temperature in the dark after being washed. The samples were then rinsed with PBS three times and treated with Vectashield (Vector Laboratories, Burlingame, CA). Target proteins were detected and visualized with fluorescence microscopy. The sections were counterstained with hematoxylin and eosin (HE). The cross-sectional area of myofibers was measured with the use of WinRoof software (version 5, Mitani, Fukui, Japan).

Semiquantitative or real-time RT-PCR. To measure the level of mRNA, semiquantitative RT-PCR was performed as described previously (13). After the synthesis of first-strand cDNAs from mRNAs, second strand synthesis and amplification of target genes were performed as described above. In this case, the PCR buffer contained two sets of primers to amplify the target gene cDNA and the internal standard glyceraldehyde-3-phosphate dehydrogenase (GAPDH) cDNA simultaneously. The sense and antisense primers used in this study are shown in Table 1. The amplification was terminated 15 min later at 72°C when PCR products were linearly amplified. The PCR products were separated by electrophoresis in an 8% PAGE and detected with a highly sensitive nucleic acid staining reagent (TaKaRa, Tokyo, Japan). The staining intensities of the target bands and internal standard gene cDNAs were estimated with an image analyzer (FMBIO II, TaKaRa), and the intensity ratio of a target gene cDNA to the internal standard gene cDNA was calculated. We used GAPDH as an internal standard gene because the denervation did not change the level of GAPDH mRNA (data not shown).

To confirm the results from the semiquantitative RT-PCR, we performed real-time RT-PCR with the same primers (Table 1) and SYBR Green dye by using a real-time PCR system (model ABI 7300, Applied Biosystems, Foster City, CA) according to the manufacturer's instruction. First-strand cDNAs were reverse transcribed at 42°C for 60 min and 95°C for 5 min from 1 μg of the extracted total RNA with Moloney murine leukemia virus reverse transcriptase (Promega) and primers (oligo-dT15 primer:random nonamer = 1:10). The reaction mixture containing reverse-transcribed cDNAs was preheated for 2 min at 50°C and for 10 min at 95°C to activate *Taq* polymerase. A 40-cycle two-step PCR was performed, consisting of 15 s at 95°C and 1 min at 60°C. The amount of target mRNA was calculated from the fractional cycle number at which the reporter fluorescence reaches a certain level. The ratio of the amounts of target mRNA to the internal standard GAPDH mRNA was shown as an arbitrary unit. Samples were amplified simultaneously in triplicate in one assay run.

Statistical analysis. All data were statistically evaluated by ANOVA with SPSS software (version 6.1; SPSS, Tokyo, Japan) and were expressed as means ± SD, $n = 3–6$. One-way ANOVA was used to determine the significant effects of denervation or osteoactivin on the measured variables. Individual differences between groups were assessed with Duncan's multiple-range test. Differences were considered significant at $P < 0.05$.

RESULTS

Denervation-stimulated expression of osteoactivin in mouse hindlimb skeletal muscles. Denervation and tail suspension for 16 days decreased the wet weight of the gastrocnemius muscle standardized by body weight to 58% and 88%, respectively, of that in the control mice (Fig. 1*A*). Semiquantitative or real-time RT-PCR for osteoactivin also showed that denervation and tail suspension increased the expression of osteoactivin mRNA by 7.1- and 2.6-fold, respectively, correlated with the decrease in wet weight of the skeletal muscle (Fig. 1*B*). This result was consistent with our previous results obtained by DNA microarray analysis for rat gastrocnemius muscle (25).

We examined whether denervation caused distinct effects on osteoactivin expression in the hindlimb skeletal muscles. Denervation decreased the standardized wet weight of all tested hindlimb skeletal muscles to the similar extent (data not shown). The amounts of osteoactivin mRNA in the fast-type skeletal muscles, including gastrocnemius and tibialis anterior muscles, gradually increased after denervation and reached the peak value on *day 10* (Fig. 1*C*). In contrast, the level of osteoactivin mRNA in the slow-type skeletal muscles, such as soleus muscle, was highest on *day 5* and then gradually decreased (Fig. 1*C*). Osteoactivin protein also accumulated in these hindlimb skeletal muscles after denervation (Fig. 1*D*). The amount of accumulated osteoactivin in the soleus muscle was sustained at the higher level during unloading, whereas the accumulation of osteoactivin protein in the gastrocnemius and tibialis anterior muscles was transient.

Denervation-mediated expression of matrix-related genes. Because denervation has been reported to induce expression of matrix-related genes, including MMPs (16), we examined expression of MMPs in the gastrocnemius muscle of denervated mice. On *day 10* after denervation, when osteoactivin protein reached the peak value, the amounts of MMP-2, -3, -9, and -14 transcripts were significantly increased in the muscle atrophied by denervation (Fig. 2*A*). Among them, the expression of MMP-3 mRNA was most significantly increased. Consistent with the increase in levels of MMP-3 and MMP-9

Table 1. *Primers for polymerase chain reaction*

Target Gene	Primer	Sequence	Length, bp
Osteoactivin	S	5′-TTCACTGTGACCTGCAAAGG-3′	161
	AS	5′-CAGTAGGTGCCAGACCCATT-3′	
MMP-2	S	5′-CACAGGAGGAGAAGGCTGTGTTCTT-3′	356
	AS	5′-GAGACTTTGGTTCTCCAGCTTCAGGT-3′	
MMP-3	S	5′-GGAAATCAGTTCTGGGCTATACGAGG-3′	301
	AS	5′-CCAACTGCGAAGATCCACTGAAGAAG-3′	
MMP-9	S	5′-TCCTACTCTGCCTGCACCACTAAAG-3′	290
	AS	5′-CTGTACCCTTGGTCTGGACAGAAAC-3′	
MMP-14	S	5′-CCCTTTTACCAGTGGATGGACACAGA-3′	298
	AS	5′-CAATGGGCATTGGGTATCCATCCATC-3′	
Atrogin-1	S	5′-GGCGGACGGCTGGAA-3′	110
	AS	5′-CAGATTCTCCTTACTGTATACCTCCTTGT-3′	
GAPDH	S	5′-ACCCAGAAGACTGTGGATGG-3′	125
	AS	5′-TTCAGCTCTGGGATGACCTT-3′	

AS, antisense; S, sense; MMP, matrix metalloproteinase; GAPDH, glyceraldehyde-3-phosphate dehydrogenase.

transcripts, denervation significantly accumulated the MMP-3 and MMP-9 proteins in gastrocnemius muscle (Fig. 2*B*). Increase in MMP-3 proteins by denervation was bigger than that of MMP-9.

Distinct expression of osteoactivin and matrix-related genes in denervated skeletal muscle. HE and Hoechst-33342 staining showed that denervation caused infiltration of mononucleated cells into the interstitial space of myofibers, whereas these cells

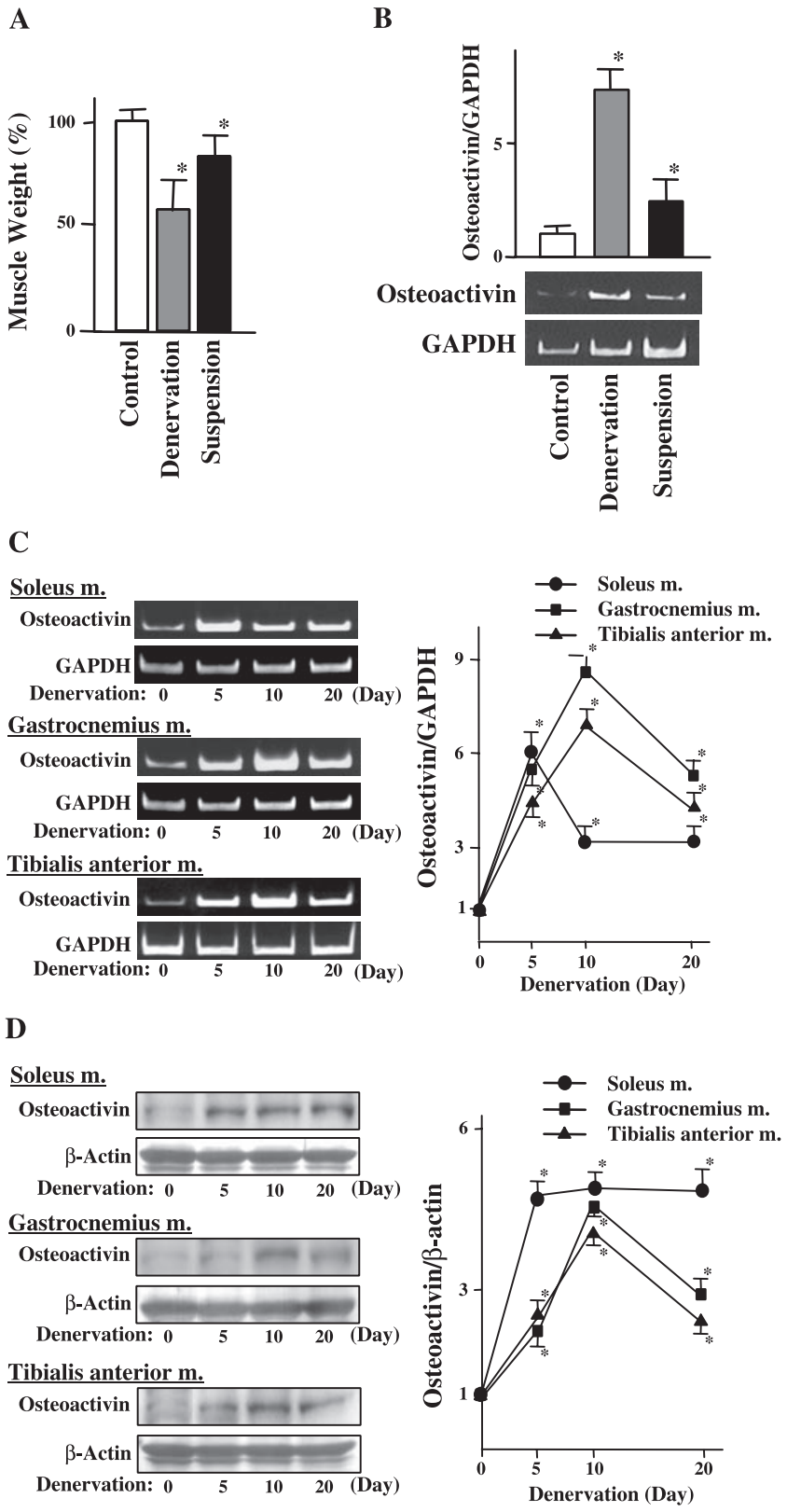

Fig. 1. Effects of denervation on osteoactivin expression in hindlimb skeletal muscles. *A*: mice (9 wk old) were subjected to 16-day denervation or tail suspension. Gastrocnemius muscle wet weight was measured after the denervation or tail suspension and was standardized by body weight. *B*: the amounts of osteoactivin and GAPDH transcripts were measured by semiquantitative RT-PCR. The intensity ratios of cDNA of osteoactivin to GAPDH were calculated. Similar results were obtained by real-time RT-PCR (data not shown). $*P < 0.05$, compared with control animals (*A* and *B*). *C*: mice (9 wk old) were subjected to denervation for the indicated period. Total RNA was extracted from the hindlimb skeletal muscles. Semiquantitative RT-PCR for osteoactivin and GAPDH were performed as described in MATERIALS AND METHODS. The intensity ratio of osteoactivin cDNA to GAPDH was calculated. Similar results were obtained by real-time RT-PCR (data not shown). *D*: proteins (40 μg/lane) prepared from the hindlimb muscles of denervated mice were subjected to SDS-8% PAGE. Immunoblotting for osteoactivin and β-actin were performed. The intensity ratio of osteoactivin protein to β-actin was calculated. Values are are means ± SD ($n = 4$) for all experiments. $*P < 0.05$, compared with the value of control muscle (*day 0*) (*C* and *D*).

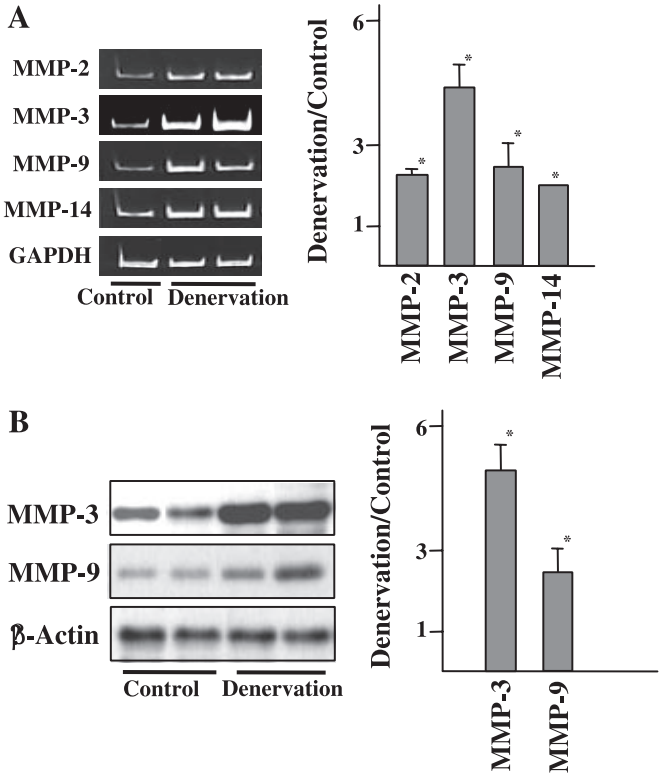

Fig. 2. Effects of denervation on expression of matrix metalloproteinases (MMPs) in mouse gastrocnemius muscle. *A*: mice (9 wk old) were subjected to denervation and euthanized on *day 10*. Control mice that underwent sham operations were prepared in parallel. The amounts of osteoactivin, MMP-2, -3, -9, and -14, or GAPDH in total RNA extracted from the gastrocnemius muscles, were quantified by using semiquantitative or real-time RT-PCR, as described in MATERIALS AND METHODS. The intensity ratio of osteoactivin cDNA to GAPDH in each group was calculated and compared with the value of control group. *B*: mice were subjected to denervation and then euthanized on *day 10*. Control mice that underwent sham operations were prepared in parallel. The levels of β-actin, MMP-3, and MMP-9 proteins were measured by immunoblot analysis. The intensity ratio of osteoactivin protein to β-actin was calculated and compared with the value of control group. Values are means ± SD ($n = 4$). *$P < 0.05$, compared with the value of control animals.

were hardly observed in the gastrocnemius muscle of tail-suspended or control mice (Fig. 3*A*). Because these cells were stained with an anti-vimentin antibody (Fig. 3*A*), they were fibroblast-like cells as reported previously (18).

We also confirmed the location of osteoactivin and MMP-3 in the gastrocnemius muscle atrophied by denervation. Mouse gastrocnemius muscle without denervation expressed very little osteoactivin or MMP-3. Interestingly, the location of MMP-3 in the denervated skeletal muscle was different from that of osteoactivin. The fibroblast-like cells were positively stained with an anti-MMP-3 antibody, whereas osteoactivin was highly expressed in the sarcolemma of myofibers adjacent to the fibroblast-like cells (Fig. 3*B*). In the denervated gastrocnemius muscle, the location of MMP-9 was similar to that of MMP-3 (data not shown).

Effects of growth factors on expression of osteoactivin protein in C_2C_{12} cells. Our anti-mouse osteoactivin antibody detected two bands of ~68- and 98-kDa molecular masses, which corresponded to nonglycosylated and glycosylated osteoactivins, respectively (28), in immunoblot analysis (Fig. 4*A*). Because only glycosylated osteoactivin responded to denervation and treatment with bFGF or PDGF, we showed the immunoblotting results of glycosylated osteoactivin below.

To examine which factors trigger expression of osteoactivin in denervated skeletal muscle, we administered bFGF and PDGF, whose expression in skeletal muscle has been reported to be upregulated by denervation (11, 27) to C_2C_{12} myoblastic cells. bFGF and PDGF significantly increased the amount of osteoactivin protein in C_2C_{12} cells (Fig. 4*B*). Heparin, which is known to inhibit bFGF-stimulated gene expression (24), inhibited expression of osteoactivin protein induced by bFGF (Fig. 4*C*).

Involvement of osteoactivin in expression of collagen type I, MMP-3, and MMP-9 in fibroblasts. To elucidate the involvement of osteoactivin in high expression of matrix-related genes in denervated skeletal muscle, we overexpressed osteoactivin in mouse C_2C_{12} myoblastic cells. We did not detect any increase in MMP expression in osteoactivin-overexpressing C_2C_{12} cells (Fig. 5*A*). In addition to myoblastic cells, we transfected osteoactivin into various cells types (data not shown), such as mouse MC3T3-E1 osteoblast-like cells and NIH-3T3 fibroblasts. Only overexpression of osteoactivin in NIH-3T3 cells significantly induced expression of MMP-3 (Fig. 5*A*). In this case, osteoactivin did not increase the amount of collagen type I, MMP-2, or MMP-9 protein (Fig. 5*A*).

To deny the possibility that overexpression of osteoactivin might artificially increase the amount of MMP-3 transcripts in fibroblasts, we treated NIH-3T3 cells with recombinant mouse osteoactivin. Recombinant osteoactivin significantly increased concentrations of collagen type I and MMP-9 as well as MMP-3 in NIH-3T3 cells, compared with the cells treated with *Lac*Z control protein (Fig. 5*B*). Consistent with the result of overexpression of osteoactivin, treatment with recombinant osteoactivin did not change expression of any tested genes in C_2C_{12} cells (data not shown). Treatment with recombinant human MMP-3 did not increase the amount of osteoactivin protein in C_2C_{12} cells (Fig. 5*B*), indicating that denervation-mediated expression of osteoactivin in muscle was not due to MMP-3 derived from fibroblasts.

Osteoactivin has two binding motifs, heparin-binding and integrin-binding motifs, in the extracellular domain (33). When two potential inhibitors for these binding motifs, heparin and RGDS peptide, were added to NIH-3T3 cells treated with recombinant osteoactivin, the former prevented osteoactivin-mediated expression of MMP-3, but the latter did not (Fig. 5*C*). Heparin also decreased levels of collagen type I and MMP-9 in NIH-3T3 cells treated with recombinant osteoactivin (data not shown). Simultaneous treatment with heparin and *Lac*Z (control protein) did not affect the amount of MMP-3 protein (data not shown).

Involvement of osteoactivin in expression of MMP-3 and MMP-9 in Schwann cells. Rich et al. (28) have recently demonstrated that osteoactivin was involved in expression of MMPs in human glioma cells. We also observed the nerve with Wallerian degeneration in the denervated skeletal muscle. Denervation caused axon and myelin breakdown in the distal neuronal segment and induced expression of osteoactivin, MMP-3, and MMP-9 in the segment (Fig. 6, and data not shown). MMP-3 and MMP-9 were highly expressed in neural cells of the segment. In contrast, denervation induced osteoactivin in Schwann-like cells (Fig. 6), which were stained with an anti-S-100 antibody (data not shown).

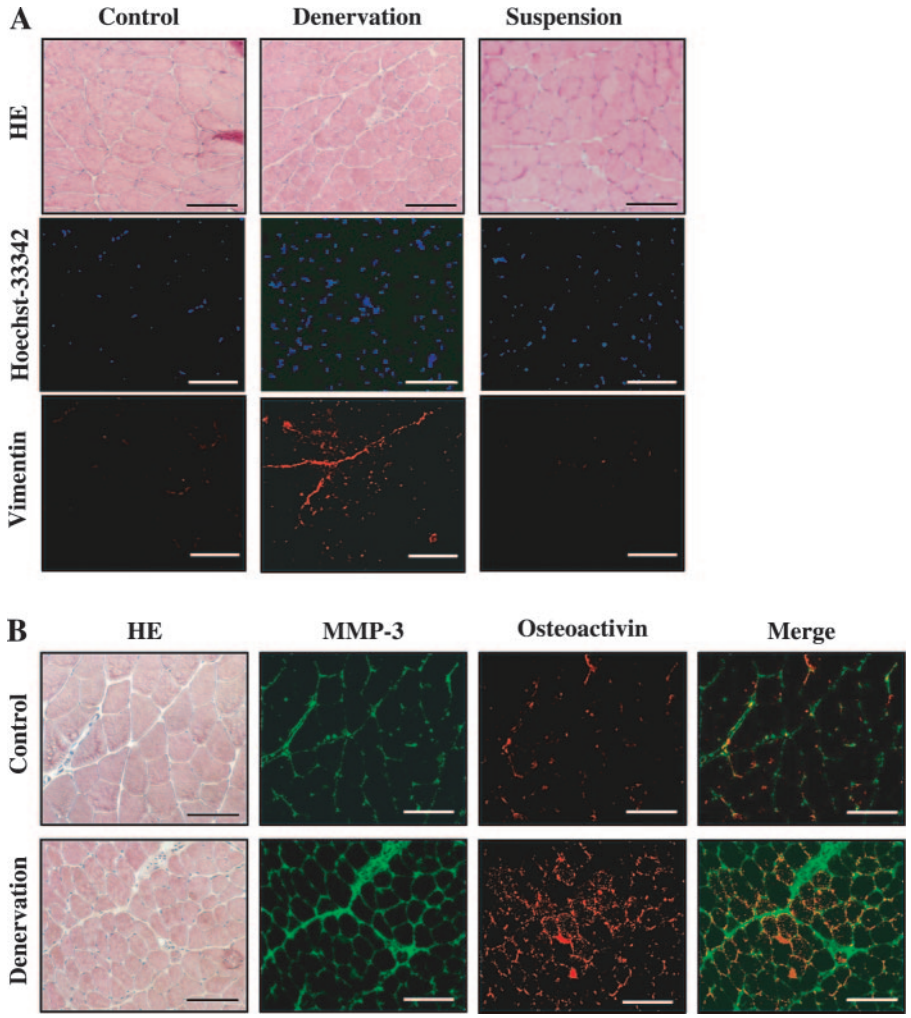

Fig. 3. Immunohistochemical analysis of MMP-3 and osteoactivin in skeletal muscle of denervated mice. *A*: sections (5 μm) from the gastrocnemius muscle of 16-day denervated ($n = 4$), 16-day tail-suspended ($n = 4$), or control mice ($n = 4$) were stained with hematoxylin and eosin (HE; *top*) or Hoechst-33342 (*middle*). The sections were also counterstained with an antibody against vimentin, a fibroblast-specific protein (*bottom*). Similar results were obtained in three separate experiments. Scale = 100 μm. *B*: mice (9 wk old, $n = 4$) were subjected to 16-day denervation four times. Control mice ($n = 4$) without denervation were prepared in parallel. The sections (5 μm) from the gastrocnemius muscle of control or denervated mice were stained with HE. The serial sections were immunostained with an anti-MMP-3 and anti-osteoactivin antibody, respectively. The images on fluorescence microscopy were merged on a personal computer. Similar results were obtained in four separate experiments, and the best results were exhibited as the representative. Scale = 100 μm.

Overexpression of osteoactivin in vivo enhanced denervation-mediated expression of MMP-3 in skeletal muscle. To define the role of osteoactivin in vivo, we created three strains of heterozygous osteoactivin-transgenic mice. Exogenous osteoactivin was confirmed to be overexpressed in gastrocnemius muscle by semiquantitative RT-PCR for osteoactivin and immunoblotting with an anti-V5 antibody (Fig. 7, *A* and *B*). Osteoactivin-transgenic mice showed no apparent abnormality (data not shown), and overexpression of osteoactivin did not change the expression of matrix-related genes, including MMP-3 in skeletal muscle at the mRNA and protein levels (Fig. 7, *A* and *B*). Interestingly, in osteoactivin-transgenic mice, denervation further enhanced expression of MMP-3 in gastrocnemius muscle, compared with wild-type mice (Fig. 7, *A* and *B*). In gastrocnemius muscle of osteoactivin-transgenic mice, the expression pattern of MMP-9 was similar to that of MMP-3 (data not shown).

Denervation decreased wet weights of gastrocnemius and soleus muscles in wild-type and osteoactivin-transgenic mice (Fig. 7*C*). However, the muscle wet weights in osteoactivin-transgenic mice were significantly bigger than those in wild-type mice on *day 20* (Fig. 7*C*). The cross-sectional area of gastrocnemius muscle fibers in denervated mice was not changed by overexpression of osteoactivin (Fig. 7*D*): the cross-sectional areas of gastrocnemius muscle fibers in wild-type and osteoactivin-transgenic mice after 16-day denervation were 990 ± 45 and 973 ± 53 μm^2, respectively. Immunohistochemical analysis of MMP-3 revealed that myofibroblasts in denervated gastrocnemius muscle of transgenic mice expressed MMP-3 protein more abundantly than those in wild-type mice (Fig. 7*D*).

Recently, several ubiquitin ligases, such as atrogin-1 (MAFbx-1) and MuRF-1, have been reported to be responsible for denervation-mediated muscle atrophy (1). To further elucidate the effects of osteoactivin on muscle proteolysis caused by denervation, we measured amounts of atrogin-1 transcripts in gastrocnemius muscle of denervated osteoactivin-transgenic mice. Denervation stimulated expression of atrogin-1 in gas-

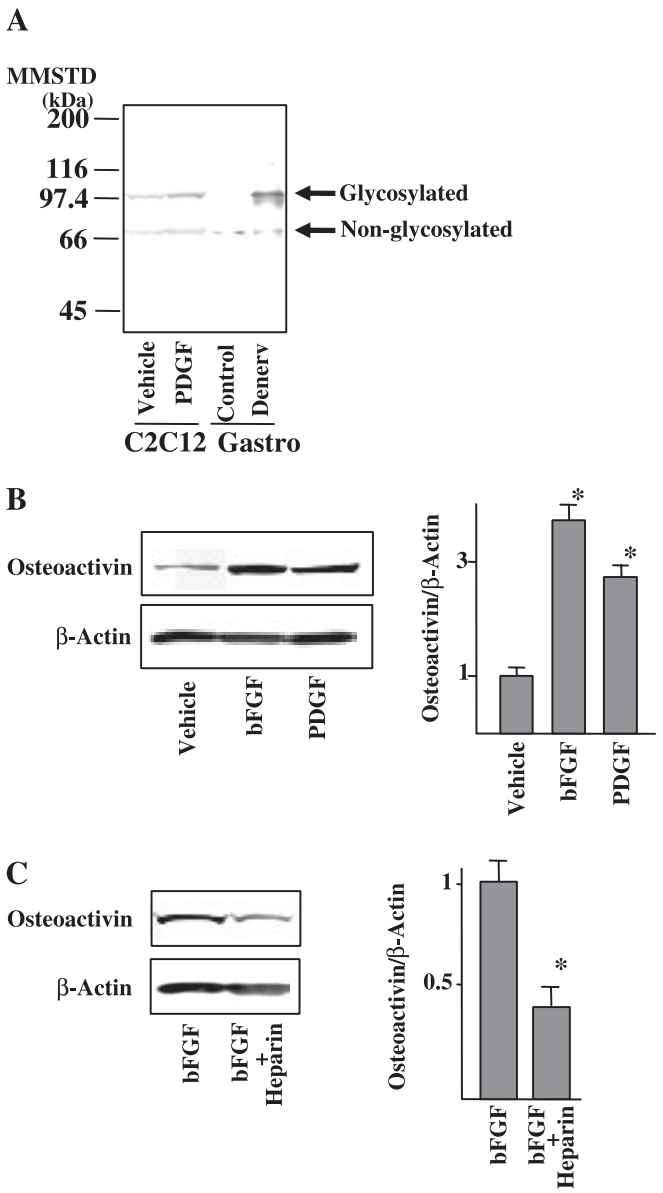

Fig. 4. Effects of basic fibroblast growth factor (bFGF) and platelet-derived growth factor (PDGF) on osteoactivin expression in C_2C_{12} cells. *A*: whole cell lysates (40 μg protein/lane) from mouse C_2C_{12} myoblastic cells treated with vehicle (PBS) or 25 ng/ml PDGF for 24 h, and homogenate (40 μg protein/lane) of the gastrocnemius muscle prepared from denervated or nondenervated (control) mice were subjected to SDS-8% PAGE. Immunoblotting was performed as described in MATERIALS AND METHODS to check our antibody against recombinant mouse osteoactivin. Gastro, gastrocnemius muscle; MMSTD, molecular mass of standards. *B*: mouse C_2C_{12} myoblastic cells of 60% confluence were treated with vehicle (PBS), 5 ng/ml of bFGF, or 25 ng/ml PDGF for 24 h. Lysates from C_2C_{12} cells (40 μg protein/lane) were subjected to SDS-8% PAGE. Immunoblotting for osteoactivin and β-actin were performed. The intensity ratio of osteoactivin protein to β-actin was calculated. Values are means ± SD ($n = 3$). *$P < 0.05$, compared with the value of vehicle-treated cells. *C*: mouse C_2C_{12} myoblastic cells of 60% confluence were treated with 5 ng/ml of bFGF in the absence or presence of 300 μg/ml heparin for 24 h. Lysates from C_2C_{12} cells (40 μg protein/lane) were subjected to SDS-8% PAGE. Immunoblotting for osteoactivin and β-actin was performed. The intensity ratio of osteoactivin protein to β-actin was calculated. Values are means ± SD ($n = 3$). *$P < 0.05$, compared with the value of bFGF-treated cells.

trocnemius muscle of wild-type mice about fourfold (Fig. 7*E*). However, overexpression of osteoactivin did not change the denervation-mediated expression of atrogin-1 (Fig. 7*E*).

DISCUSSION

Denervation occasionally induced expression of MMPs, such as MMP-2 and MMP-9, in skeletal muscle (16), although the molecular mechanism of the MMP expression caused by denervation is still unknown. The present study suggests a novel molecule for mediating the interaction between the muscle fibers and interstitial fibroblasts. Denervation induced the expression of osteoactivin in the sarcolemma of myofibers. Treatment with osteoactivin or its overexpression induced expression of matrix-related genes in fibroblasts, whereas MMP-3 did not change expression of osteoactivin in myoblasts. Our results suggest that denervation-induced osteoactivin in myofibers might function as an activator for fibroblasts to induce expression of collagen type I, MMP-3, and MMP-9.

To elucidate whether osteoactivin influences denervation-induced myolysis, we have measured the mass (wet weight and cross-sectional area) of hindlimb skeletal muscles and expression of atrogin-1, a muscle atrophy-related gene (1), in gastrocnemius muscle of osteoactivin-transgenic mice. In osteoactivin-transgenic mice, denervation significantly increased wet weights of gastrocnemius and soleus muscles compared with those in wild-type mice, whereas the cross-sectional area of gastrocnemius muscle was not changed. In addition, denervation significantly increased expression of atrogin-1, as described by Bodine et al. (1). However, in vivo overexpression of osteoactivin did not affect this denervation-mediated induction of atrogin-1. These findings suggest that in vivo overexpression of osteoactivin might not change denervation-mediated muscle atrophy, but increase volumes of interstitial spaces between muscle fibers.

In osteoactivin-transgenic mice without denervation, high expression of matrix-related genes was not observed in hindlimb skeletal muscle. Only in denervated skeletal muscle did osteoactivin stimulate expression of MMP-3 in myofibroblasts. Denervation-mediated activation of myofibroblasts might be multistep reactions and require other factors, such as inducers for infiltration of fibroblasts into the skeletal muscles.

Treatment with recombinant osteoactivin increased the amounts of MMP-3, MMP-9, and collagen type I in NIH-3T3 fibroblasts. MMP-3 has been reported to regulate growth and development of tissues by selective degradation of insulin-like growth factor-I (IGF-1)/IGF-1-binding protein complexes (9). Secreted MMP-9 is also involved in the migration and myotube formation of myoblastic cells (17). Furthermore, targeted disruption of the MMP-3 gene in mice caused a delay in wound healing due to a failure in fibroblast contraction (2, 3). Synthetic MMP inhibitors undergoing clinical trials had reversible musculoskeletal toxicity as the main side effect (14). On the basis of these findings, an osteoactivin-mediated increase in MMPs in skeletal muscle might be useful for regeneration or degeneration in the denervated skeletal muscle, leading to compensation for the loss of muscle volume or protection of muscle fibers against injury after denervation.

Recombinant osteoactivin truncated the COOH-terminal domain (intracellular domain) was used in this study, because a full-length osteoactivin expressed in *E. coli* was quite insoluble

(data not shown). In addition, overexpression of the truncated osteoactivin had effects on fibroblasts similar to those of full-length osteoactivin (data not shown). Therefore, we focused on the extracellular domain of osteoactivin as a functional site. Osteoactivin has two functional motifs in the extracellular domain: a heparin-binding motif and an RGD motif for an integrin-binding site (33). In fibroblasts treated with recombinant osteoactivin, an integrin inhibitor did not suppress expression of collagen type I, MMP-3, or MMP-9, whereas heparin significantly canceled osteoactivin-mediated expression of these proteins. These findings strongly suggest that osteoactivin affects fibroblasts via a heparin-binding motif, but not via an integrin-binding motif. Fibroblasts highly expressing heparan sulfate proteoglycans have been reported to be proliferated near denervated synaptic sites in the skeletal muscle (10). The interaction between osteoactivin in myocytes and heparan sulfate proteoglycan on the surface of infiltrated fibroblasts might play an important role in regulating functions of fibroblasts in the interstitial spaces of the denervated skeletal muscle. Identifying a proteoglycan (receptor) specifically binding to osteoactivin is the next and ongoing important subject.

Because osteoactivin has been reported to be involved in expression of MMPs in human glioma cells (28), we also examined the expression of osteoactivin and MMPs in neurectomized neurons. Osteoactivin was overexpressed in Schwann-like cells in neurons with Wallerian degeneration, whereas MMP-3 and MMP-9 were present in neuronal cells in the neurectomized sciatic nerve. In neurons, osteoactivin expressed in Schwann-like cells might induce expression of MMP-3 in neuronal cells. Upregulation of MMPs, such as MMP-2 and MMP-9, during denervation has been reported to enable axonal regrowth by removal of inhibitory factors from the basal lamina of Schwann cells (8). Therefore, it is likely that in the nerve system, osteoactivin might function as an activator for connective cells and facilitate the regeneration of neurons by secretion of MMP-3 and MMP-9 from axons in the vicinity of Schwann cells.

Expression of osteoactivin has been reported to be upregulated in osteoblasts of rats with osteopetrosis or in hepatocytes of rats with liver cirrhosis. However, the factors that trigger expression of osteoactivin are little known. In skeletal muscles and neurons during denervation, the expression of bFGF and PDGF has been reported to be upregulated (11, 27). In this study, we found that bFGF and PDGF significantly induced expression of osteoactivin in skeletal muscle cells. Heparin, an antagonist of bFGF, significantly inhibited bFGF-mediated expression of osteo-

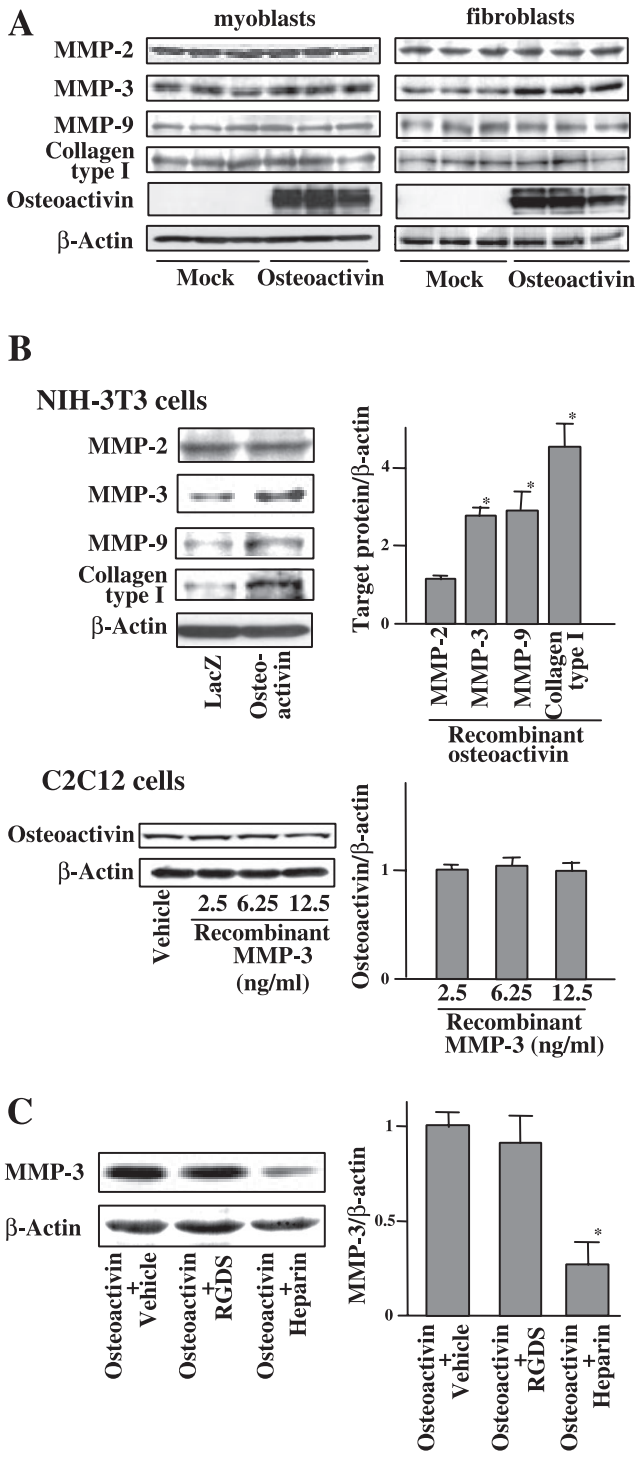

Fig. 5. Effects of overexpression or treatment of osteoactivin on MMPs and collagen type I in C_2C_{12} myoblasts or NIH-3T3 fibroblasts. *A*: C_2C_{12} or NIH-3T3 cells were transfected with a mock vector (pcDNA 3.1V5/His) or the purified plasmid containing V5-tagged full-length mouse osteoactivin. After 48-h culturing, the amounts of collagen type I, osteoactivin, β-actin, and MMP-2, -3, and -9 proteins in these transfected cells were estimated by immunoblotting with respective antibodies. Only osteoactivin was detected by immunoblotting with an anti-V5 antibody. Similar results were obtained in 3 separate experiments. *B*: recombinant *LacZ* or mouse COOH-terminal-truncated osteoactivin was purified as described in MATERIALS AND METHODS. NIH-3T3 cells (60% of confluence) were treated with 25 nM of the purified recombinant *LacZ* or osteoactivin for 24 h. In contrast, C_2C_{12} cells were treated with recombinant human MMP-3 at the indicated concentration for 24 h. Whole cell extracts (40 μg protein/lane) were subjected to immunoblot analysis for collagen type I, β-actin, osteoactivin, MMP-2, MMP-3, and MMP-9. The intensity ratios of interest proteins to β-actin were calculated, and the value of cells treated with *LacZ* was shown as one arbitrary unit. The data are means ± SD ($n = 4$). *$P < 0.05$, compared with the value of control treatment. *C*: NIH-3T3 cells were also treated with vehicle, 100 μM RGDS peptide, or 300 μg/ml heparin, in addition to 25 nM recombinant COOH-terminal-truncated osteoactivin. After 24-h culturing, whole cell extracts (40 μg protein/lane) were subjected to immunoblot analysis for MMP-3. The intensity ratio of MMP-3 protein to β-actin was calculated. Values are means ± SD ($n = 3$). *$P < 0.05$, compared with the value of osteoactivin treatment.

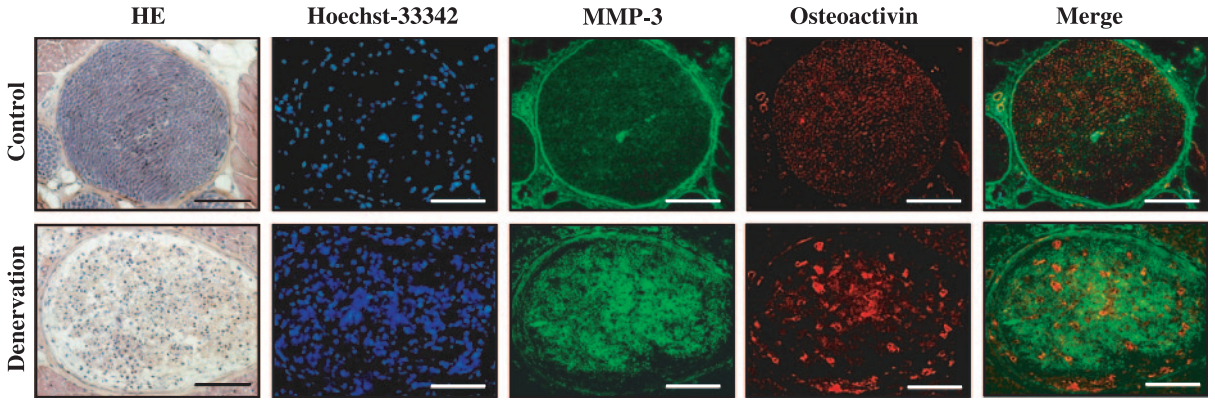

Fig. 6. Immunohistochemical analysis of MMP-3 and osteoactivin in neurectomized neurons. Mice (9 wk old, $n = 4$) were subjected to 16-day denervation four times. Control mice (9 wk old, $n = 4$) without denervation were prepared in parallel. The sections (5 μm) from the neuron in gastrocnemius muscle of control or denervated mice were stained with HE or Hoechst-33342. The serial sections were immunostained with an anti-MMP-3 and anti-osteoactivin antibody, respectively. The images obtained using fluorescence microscopy were merged on a personal computer. Similar results were obtained in four separate experiments, and the best results were exhibited as the representative. Scale = 100 μm.

activin protein, strongly suggesting that in denervated skeletal muscle, expression of osteoactivin might be regulated by these denervation-derived growth factors, especially bFGF. These results were supported by the study of Dell'Era et al. (7) that in macroarray analysis of bFGF-transformed endothelial cells, expression of osteoactivin was remarkably upregulated. Recently, it has been reported that in the liver of bFGF-deficient mice, liver fibrosis caused by exposure to

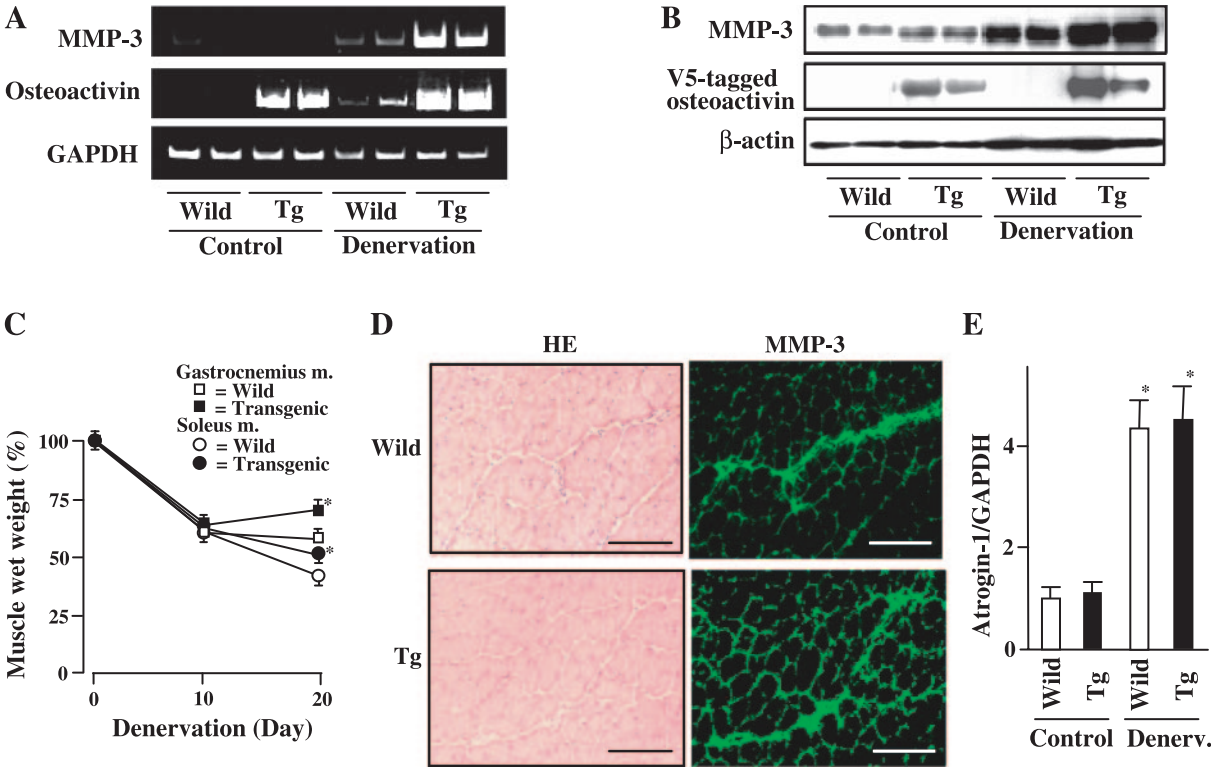

Fig. 7. Effect of denervation on MMP-3 expression in hindlimb skeletal muscles of osteoactivin-transgenic mice. *A*: wild-type (wild) or osteoactivin-transgenic (Tg) mice (9 wk old) were subjected to 16-day denervation (Denerv). Control mice that underwent sham operations were prepared in parallel. Total RNA was extracted from the gastrocnemius muscle. Semiquantitative RT-PCR for osteoactivin and GAPDH were performed as described in MATERIALS AND METHODS. Similar results were obtained by real-time RT-PCR (data not shown). *B*: proteins (40 μg/lane) prepared from the gastrocnemius muscles of denervated or control mice were subjected to SDS-8% PAGE. Immunoblotting for MMP-3, V5/His-tagged osteoactivin, and β-actin were performed. Similar results were obtained in four separate experiments. *C*: wild-type and osteoactivin-transgenic mice were subjected to denervation. Wet muscle weight per kilogram body weight in denervated animals at the indicated times was expressed as a percentage weight reduction relative to control animals. The results are shown as means ± SD ($n = 5$). *$P < 0.05$, compared with the values of wild-type mice. *D*: section (5 μm) from the gastrocnemius muscle of 16-day denervated wild-type ($n = 3$) or osteoactivin-transgenic mice ($n = 3$) were stained with an antibody against MMP-3. The sections were also counterstained with HE. Similar results were obtained in 3 separate experiments, and the best results were exhibited as the representative. Scale = 100 μm. *E*: total RNA was extracted from the gastrocnemius muscle of 16-day denervated ($n = 3$) or control mice ($n = 3$). Real-time RT-PCR for atrogin-1 was performed as described in MATERIALS AND METHODS. The ratio of atrogin-1 to GAPDH was calculated and compared with the value of wild-type mice. Values are means ± SD ($n = 3$). *$P < 0.05$, compared with the value of wild-type mice.

chronic carbon tetrachloride was remarkably decreased (38). Osteoactivin might play an important role in fibrosis in such diseases. Further examinations are required to elucidate this hypothesis.

In general, unloading, such as spaceflight, tail suspension, and denervation, preferentially affects slow-twitch skeletal muscles more than fast-twitch skeletal muscles. For example, the regulation of skeletal muscle genes by denervation contrasted between the two types of skeletal muscles, although denervation caused an increase in UCP3 mRNA levels in both types of muscles (15). Denervation also caused slow to fast transformation in rat soleus muscle (20). Our present finding that soleus muscle sustained a much prolonged increase in the level of osteoactivin, compared with gastrocnemius muscle, was consistent with these previous reports, although the detailed mechanism of distinct osteoactivin expression in soleus and gastrocnemius muscles are unknown at this present. However, histochemical analysis of osteoactivin in soleus muscle showed a pattern similar to that in gastrocnemius muscle, except for the expression period (data not shown), indicating that osteoactivin expressed in soleus and gastrocnemius muscle has similar physiological roles.

This study provides the first evidence that osteoactivin is a novel activator of fibroblasts in denervated skeletal muscle. Development of agents for regulating the osteoactivin function is ongoing and will be an important step to further elucidate the physiological function of fibroblasts for regeneration or degeneration in extracellular matrix after denervation.

ACKNOWLEDGMENTS

We thank Dr. N. Harada, The University of Tokushima School of Medicine, Tokushima, Japan, for kindly providing NIH-3T3 cells.

GRANTS

This work was supported by the Sasakawa Scientific Research Grant from The Japan Science Society (to T. Ogawa) and Japan Aerospace Exploration Agency and Japan Space Forum Grants-in-Aid of "Ground Research Announcement for Space Utilization" (to T. Nikawa and N. Yasui).

REFERENCES

1. **Bodine SC, Latres E, Baumhuester S, Lai VKM, Nunez L, Clarke BA, Poueymirou WT, Panaro FJ, Na E, Dharmarajan K, Pan ZQ, Valenzuela DM, DeChiara TM, Stitt TN, Yancopoulos GD, and Glass DJ.** Identification of ubiquitin ligases required for skeletal muscle atrophy. *Science* 294: 1704–1708, 2001.
2. **Bullard KM, Mudgett JS, Scheuenstuhl H, Hunt TK, and Banda MJ.** Stromelysin-1-deficient fibroblasts display impaired contraction in vitro. *J Surg Res* 84: 31–34, 1999.
3. **Bullard KM, Lund L, Mudgett JS, Werb Z, Mellin JN, Hunt TK, Murphy B, Ronan J, and Banda MJ.** Impaired wound contraction in stromelysin-1 deficient mice. *Ann Surg* 230: 260–265, 1999.
4. **Cheng C and Shuman S.** Recombinogenic flap ligation pathway for intrinsic repair of topoisomerase IB-induced double-strand breaks. *Mol Cell Biol* 20: 8059–8068, 2000.
5. **Chomczynski P and Mackey K.** Modification of the TRI reagent procedure for isolation of RNA from polysaccharide- and proteoglycan-rich sources. *Biotechniques* 19: 942–945, 1995.
6. **Connor EA and McMahan UJ.** Cell accumulation in the junctional region of denervated muscle. *J Cell Biol* 104: 109–120, 1987.
7. **Dell'Era P, Coco L, Ronca R, Sennino B, and Presta M.** Gene expression profile in fibroblast growth factor 2-transformed endothelial cells. *Oncogene* 21: 2433–2440, 2002.
8. **Ferguson TA and Muir D.** MMP-2 and MMP-9 increase the neurite-promoting potential of Schwann cell basal laminae and are upregulated in degenerated nerve. *Mol Cell Neurosci* 16: 157–167, 2000.
9. **Fowlkes JL, Serra DM, Bunn RC, Thrailkill KM, Enghild JJ, and Nagase H.** Regulation of insulin-like growth factor (IGF)-I action by matrix metalloproteinase-3 involves selective disruption of IGF-I/IGF-binding protein-3 complexes. *Endocrinology* 145: 620–626, 2004.
10. **Gatchalian CL, Schachner M, and Sanes JR.** Fibroblasts that proliferate near denervated synaptic sites in skeletal muscle synthesize the adhesive molecules tenascin (J1), N-CAM, fibronectin, and a heparan sulfate proteoglycan. *J Cell Biol* 108: 1873–1890, 1989.
11. **Grothe C, Meisinger C, and Claus P.** In vivo expression and localization of the fibroblast growth factor system in the intact and lesioned rat peripheral nerve and spinal ganglia. *J Comp Neurol* 434: 342–357, 2001.
12. **Hellgren I, Drvota V, Pieper R, Enoksson S, Blomberg P, Islam KB, and Sylven C.** Highly efficient cell-mediated gene transfer using non-viral vectors and FuGene6: in vitro and in vivo studies. *Cell Mol Life Sci* 57: 1326–1333, 2000.
13. **Ikemoto M, Nikawa T, Takeda S, Watanabe C, Kitano T, Baldwin KM, Izumi R, Nonaka I, Towatari T, Teshima S, Rokutan K, and Kishi K.** Space shuttle flight (STS-90) enhances degradation of rat myosin heavy chain in association with activation of ubiquitin-proteasome pathway. *FASEB J* 15: 1279–1281, 2001.
14. **Jabs T, Tschope M, Colling C, Hahlbrock K, and Scheel D.** Elicitor-stimulated ion fluxes and O_2^- from the oxidative burst are essential components in triggering defense gene activation and phytoalexin synthesis in parsley. *Proc Natl Acad Sci USA* 94: 4800–4805, 1997.
15. **Kontani Y, Wang Z, Furuyama T, Sato Y, Mori N, and Yamashita H.** Effects of aging and denervation on the expression of uncoupling proteins in slow- and fast-twitch muscles of rats. *J Biochem (Tokyo)* 132: 309–315, 2002.
16. **Kherif S, Dehaupas M, Lafuma C, Fardeau M, and Alameddine HS.** Matrix metalloproteinases MMP-2 and MMP-9 in denervated muscle and injured nerve. *Neuropathol Appl Neurobiol* 24: 309–319, 1998.
17. **Lewis MP, Tippett HL, Sinanan AC, Morgan MJ, and Hunt NP.** Gelatinase-B (matrix metalloproteinase-9; MMP-9) secretion is involved in the migratory phase of human and murine muscle cell cultures. *J Muscle Res Cell Motil* 21: 223–233, 2000.
18. **Li Y, Foster W, Deasy BM, Chan Y, Prisk V, Tang Y, Cummins J, and Huard J.** Transforming growth factor-β1 induces the differentiation of myogenic cells into fibrotic cells in injured skeletal muscle: a key event in muscle fibrogenesis. *Am J Pathol* 164: 1007–1019, 2004.
19. **Lowry OH, Rosebrough NJ, Farr AL, and Randall RJ.** Protein measurement with the Folin phenol reagent. *J Biol Chem* 193: 265–275, 1951.
20. **Midrio M, Danieli-Betto D, Megighian A, Velussi C, Catani C, and Carraro U.** Slow-to-fast transformation of denervated soleus muscle of the rat, in the presence of an antifibrillatory drug. *Pflügers Arch* 420: 446–450, 1992.
21. **Murray MA and Robbins N.** Cell proliferation in denervated muscle: time course, distribution and relation to disuse. *Neuroscience* 7: 1817–1822, 1982.
22. **Murray MA and Robbins N.** Cell proliferation in denervated muscle: identity and origin of dividing cells. *Neuroscience* 7: 1823–1833, 1982.
23. **Musacchia XJ, Steffen JM, and Fell RD.** Disuse atrophy of skeletal muscle: animal models. *Exerc Sport Sci Rev* 16: 61–87, 1988.
24. **Newman DR, Li CM, Simmons R, Khosla J, and Sannes PL.** Heparin affects signaling pathways stimulated by fibroblast growth factor-1 and -2 in type II cells. *Am J Physiol Lung Cell Mol Physiol* 287: L191–L200, 2004.
25. **Nikawa T, Ishidoh K, Hirasaka K, Ishihara I, Ikemoto M, Kano M, Kominami E, Nonaka I, Ogawa T, Adams GR, Baldwin KM, Yasui N, Kishi K, and Takeda S.** Skeletal muscle gene expression in space-flown rats. *FASEB J* 18: 522–524, 2004.
26. **Onaga M, Ido A, Hasuike S, Uto H, Moriuchi A, Nagata K, Hori T, Hayashi K, and Tsubouchi H.** Osteoactivin expressed during cirrhosis development in rats fed a choline-deficient, L-amino acid-defined diet, accelerates motility of hepatoma cells. *J Hepatol* 39: 779–785, 2003.
27. **Oya T, Zhao YL, Takagawa K, Kawaguchi M, Shirakawa K, Yamauchi T, and Sasahara M.** Platelet-derived growth factor-β expression induced after rat peripheral nerve injuries. *Glia* 38: 303–312, 2002.
28. **Rich JN, Shi Q, Hjelmeland M, Cummings TJ, Kuan CT, Bigner DD, Counter CM, and Wang XF.** Bone-related genes expressed in advanced malignancies induce invasion and metastasis in a genetically defined human cancer model. *J Biol Chem* 278: 15951–15957, 2003.

29. **Rosado-Ruiz T, Antommattei-Perez FM, Cadilla CL, and Lopez-Garriga J.** Expression and purification of recombinant hemoglobin I from *Lucina pectinata*. *J Protein Chem* 20: 311–315, 2001.
30. **Safadi FF, Xu J, Smock SL, Rico MC, Owen TA, and Popoff SN.** Cloning and characterization of osteoactivin, a novel cDNA expressed in osteoblasts. *J Cell Biochem* 84: 12–26, 2001.
31. **Sakai K and Miyazaki J.** A transgenic mouse line that retains Cre recombinase acitivity in mature oocytes irrespective of the Cre transgene transmission. *Biochem Biophys Res Commun* 237: 318–324, 1997.
32. **Salonen V, Lehto M, Kalimo M, Penttinen R, and Aro H.** Changes in intramuscular collagen and fibronectin in denervation atrophy. *Muscle Nerve* 8: 125–131, 1985.
33. **Shikano S, Bonkobara M, Zukas PK, and Ariizumi K.** Molecular cloning of a dendritic cell-associated transmembrane protein, DC-HIL, that promotes RGD-dependent adhesion of endothelial cells through recognition of heparan sulfate proteoglycans. *J Biol Chem* 276: 8125–8134, 2001.
34. **Smith DB and Johnson KS.** Single-step purification of polypeptides expressed in *Escherichia coli* as fusions with glutathione S-transferase. *Gene* 67: 31–40, 1988.
35. **Steinbuch M and Audran R.** The isolation of IgG from mammalian sera with the aid of caprylic acid. *Arch Biochem Biophys* 134: 279–284, 1969.
36. **Weterman MA, Ajubi N, van Dinter IM, Degen WG, van Muijen GN, Ruitter DJ, and Bloemers HP.** Nmb, a novel gene, is expressed in low-metastatic human melanoma cell lines and xenografts. *Int J Cancer* 60: 73–81, 1995.
37. **Wronski TJ and Morey-Holton ER.** Skeletal response to simulated weightlessness: a comparison of suspension techniques. *Aviat Space Environ Med* 58: 63–68, 1987.
38. **Yu C, Wang F, Jin C, Huang X, Miller DL, Basilico C, and McKeehan WL.** Role of fibroblast growth factor type 1 and 2 in carbon tetrachloride-induced hepatic injury and fibrogenesis. *Am J Pathol* 163: 1653–1662, 2003.